On Line Supplement:

The following is a detailed description of the methods used for cardiac segmentation of the heart on CT scan. A detailed atlas and spatial-temporal statistical model of the human heart was applied as the shape model describing the heart structure. This model is based on a large population of 3D+time multi-slice computed tomography sequences (138 subjects) drawn from a variety of pathologies.

The atlas is fit to the image by means of an active shape model [23] which characterizes the heart as a column vector of coordinates $\boldsymbol{s} = (x_1, y_1, z_1, \ldots, x_n, y_n, z_n)^{\mathrm{T}}$. These coordinates represent a statistical model described by its first order statistic, the average $\bar{\boldsymbol{s}}$, and the second order statistic, the variance $\boldsymbol{\Phi}$. Thus, the resulting representation becomes:

$$\boldsymbol{s} = \bar{\boldsymbol{s}} + \boldsymbol{\Phi}\mathbf{b} \qquad (1)$$

where $\mathbf{b}$ is the corresponding coefficient vector of a smaller dimension than $\boldsymbol{s}$ that explains 95% of the total variance of the data. The statistical model considers 50 modes of variation to describe the non-affine deformations of the heart, i.e. the dimension of $\mathbf{b}$ is 50 and the information provided by the statistical model is $\bar{\boldsymbol{s}}$ and $\boldsymbol{\Phi}$.

The segmentation process begins with a manual initialization of the preliminary fitting, $\bar{\boldsymbol{s}}$, followed by automated iteration to optimize surface identification and labeling.

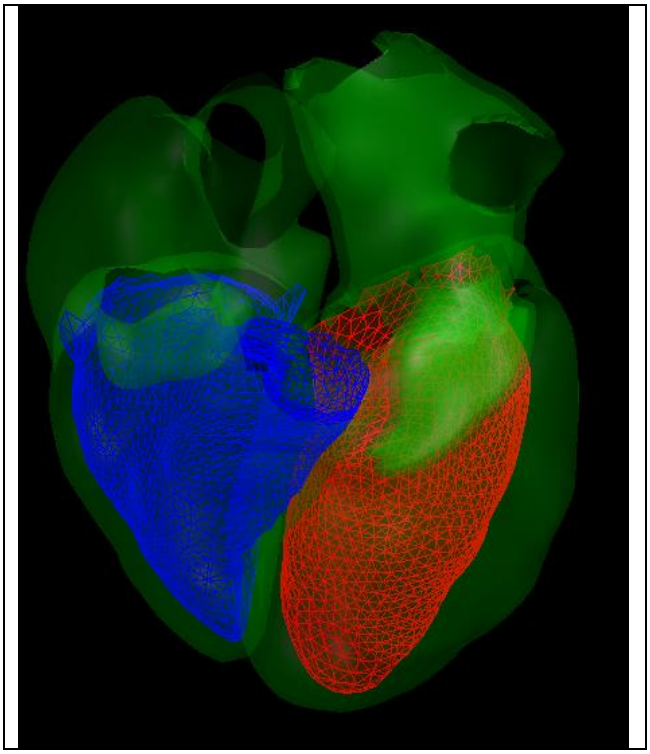

Figure 1S: Multi cavity Shape Model

The user is presented with the CT scan and a 3D rendering of the multi cavity shape model illustrated in **Figure 1S**. This shape model is then manually placed in the centroid of the heart by means of an in-house application shown in **Figure 2S** where the CT image is represented in axial, coronal, and saggital slices and the heart model is shown as a 3D mesh.

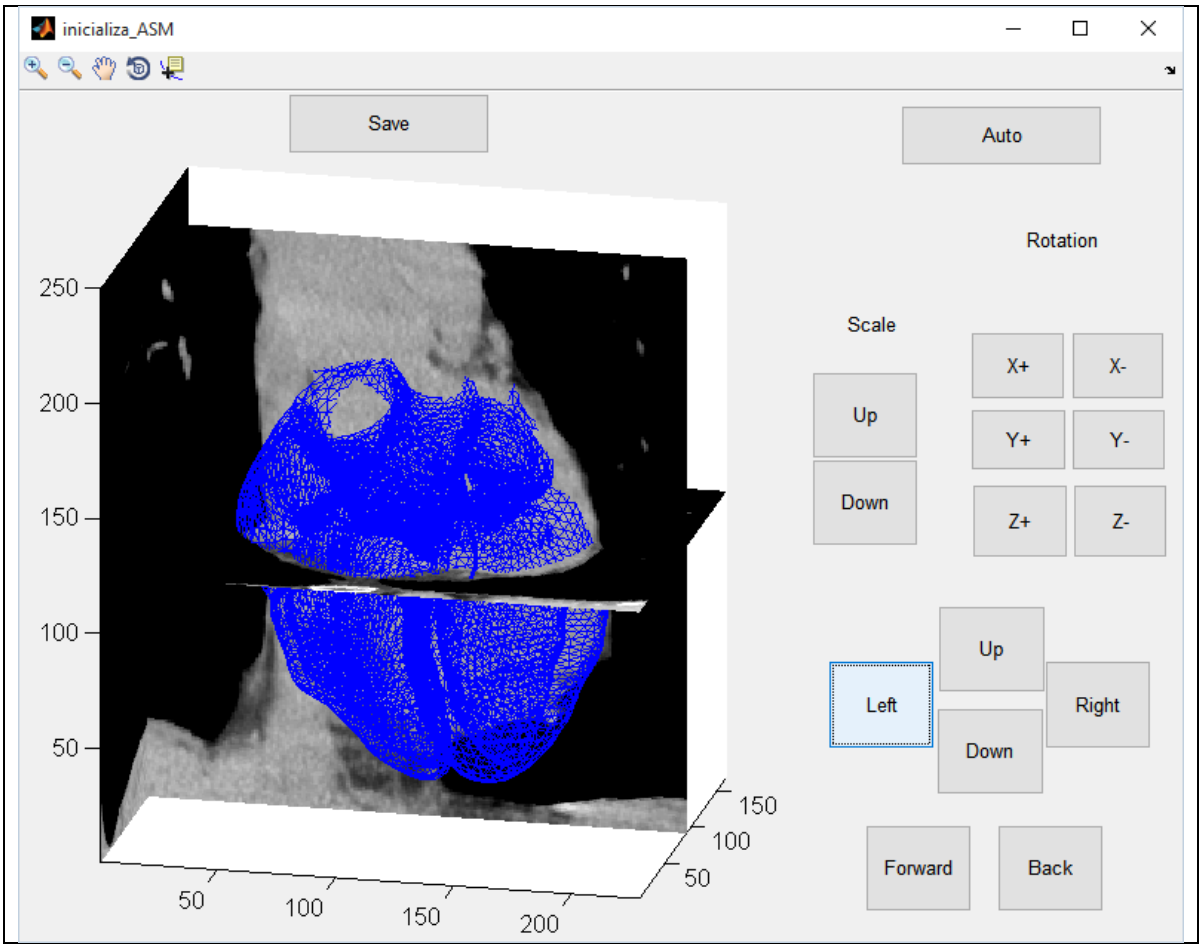

Figure 2S: Interface of the initialization application

The operator can perform affine transformations (6 degrees of freedom plus scale) to the model to adapt its initial pose to the heart structures visualized on an individual CT scan. This is done by changing the rotation, scale, and displacement of the model in the X, Y, and Y axis of the scan.

The surface fitting is also assisted by a "probabilistic driven initialization" to determine the boundary between pericardial fat and myocardium. This mode selects vertices in a direction which is orthogonal to the manually initialized surface and examines the distribution of the attenuation values along those vertices in a window from -200 to 200 HU. **Figure 3S** demonstrates the automatic detection of vertices after one iteration of the probabilistic driven initialization (pressing "Auto button"). Note that the green points automatically delineate the boundaries of the epicardial surface with respect lung and pericardial fat, the information provided by the detected vertices is used to calculate the most suitable parameters of the affine transformation by means of Horn's quaternion-based algorithm [24] for calculating the absolute orientation (pose and scale) of the shape model.

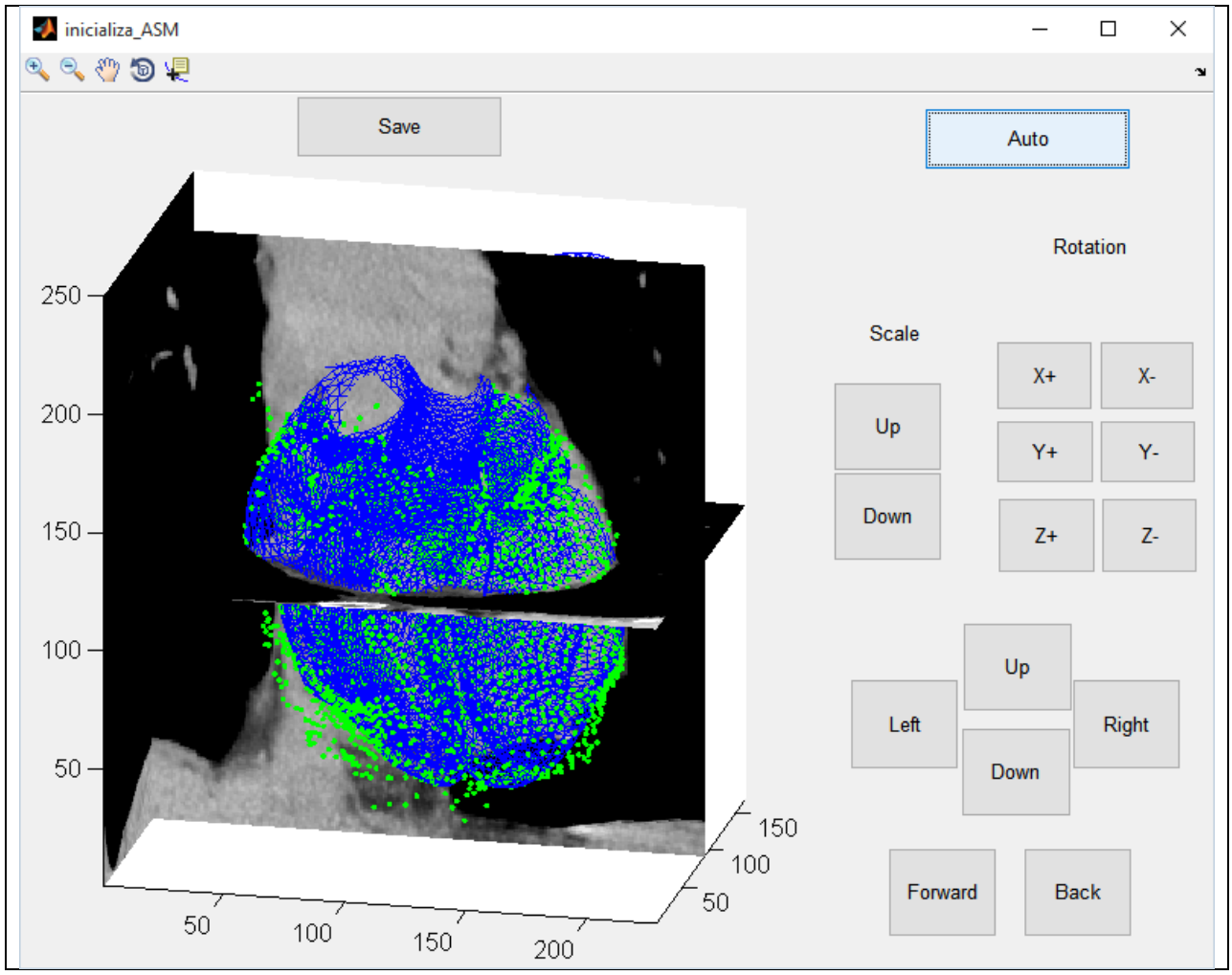

Figure 3S: Automatic location of vertices

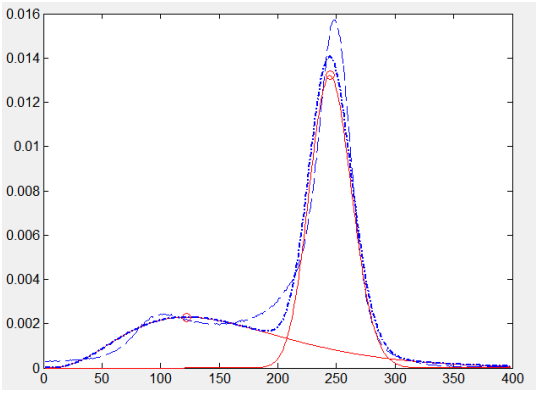

Figure 4S: Statistical characterization of tissues.

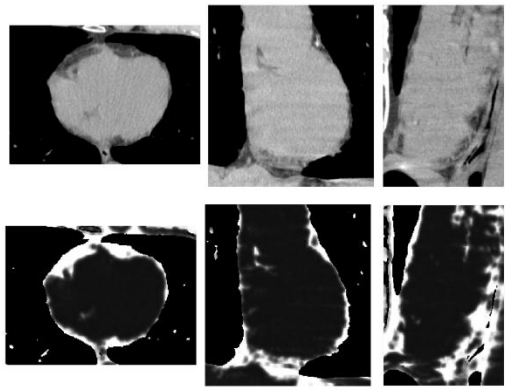

Figure 5S: Top: Gray scale image of the heart. Attenuation maps in the window [-200, 200] HUs. Bottom: Components of the heart labeled as being pericardial fat (white) or myocardium/muscle (black).

An example of the HU distributions is shown in **Figure 4S**. Based on the assumption that there are two tissues present in a single pathway (pericardial fat and then myocardium as one travels the path towards the centroid of the heart), one can fit a mixture of two components of non-central Gamma distributions in the attenuation window, where the lower distribution represents pericardial fat and the higher distribution represents the blood/muscle attenuation (**Figure 5S**).

This family of parametric distributions was selected because they include the qualitative behavior commonly shown in CT scanners: 1) skewness to higher attenuation levels; 2) myocardial tissue shows attenuation higher than -200 HU and approximates -200 HU with a derivative of higher order than 1 (smoothly). The histogram of myocardial tissue (**Figure 4S**) illustrates these characteristics. This qualitative behavior can be effectively described by means of the non-central Gamma (nc-Gamma) distribution, whose PDF is defined as follows:

$$f_X(x;\alpha,\beta,\delta) = \frac{(x-\delta)^{\alpha-1}}{\Gamma(\alpha)\beta^{\alpha}} e^{-\frac{x-\delta}{\beta}}, \quad with\ x \geq \delta \qquad (2)$$

where δ is the location parameter, α accounts for the shape and β for the scale and $\Gamma(\cdot)$ is the Euler's Gamma function.

The mixture of Gamma distributions is calculated by means the Expectation-Maximization algorithm as described previously [25, 26]: Let $X = \{x_i\}, 1 \leq i \leq N$ be independent and identically distributed random variables following the aforementioned n-c Gamma distribution (attenuation levels of the CT image centered in -200 HU). The mixture model attributes these variables to contributions of J distributions $p(x|\boldsymbol{\Theta}) = \sum_{j=1}^{J} \pi_j f_X(x;\alpha_j,\beta_j,\delta_j)$, where $\boldsymbol{\Theta}$ is a vector of the parameters of the mixture model (π_j, Θ_j) and Θ_j are the parameters of the PDF, $\Theta_j = (\alpha_j,\beta_j,\delta_j)$. Finally, $\sum_{j=1}^{J} \pi_j = 1$ must hold to guarantee that f_X is a true probability density.

The methodology applied for estimating the parameters of the mixture model is as follows:

1. **Initialization.** A first estimate of the hidden variables is obtained by clustering the data with the k-means algorithm. For each cluster, parameters $\widehat{\Theta}_j$ and $\widehat{\pi}_j$ are estimated from the samples as the maximum likelihood of each component separately.

2. **Bayesian Inference.** The probability of belonging to each tissue class is calculated for each voxel:

$$\gamma_{i,j} = p\left(Z_i = j | x_i, \widehat{\Theta}_{\mathrm{j}}\right) = \frac{\widehat{\pi}_{\mathrm{j}} \mathrm{p}(x_i, \widehat{\Theta}_{\mathrm{j}})}{\mathrm{p}(x_i | \widehat{\Theta}_{\mathrm{j}})} \quad (3)$$

where Z_i accounts for the hidden random variable whose value indicates the tissue in which the attenuation level x_i is classified (1 stands for pericardial fat and 2 for myocardial tissue).

3. **Expectation-Maximization step.** The estimate for $\widehat{\Theta}_{\mathrm{j}}$ and $\widehat{\pi}_{\mathrm{j}}$ are calculated by the following equations already derived in [references 7 and 8 of the previous footnotes]:

$$\log(\hat{\alpha}_j) - \psi(\hat{\alpha}_j) = \log\left(\frac{\sum_{i=1}^{N} \gamma_{i,j} x_i}{\sum_{i=1}^{N} \gamma_{i,j}}\right) - \frac{\sum_{i=1}^{N} \gamma_{i,j} \log(x_i)}{\sum_{i=1}^{N} \gamma_{i,j}} \quad (4)$$

$$\widehat{\pi}_{\mathrm{j}} = \frac{1}{\mathrm{N}} \sum_{i=1}^{N} \gamma_{i,j} \quad (5)$$

$$\hat{\beta}_{\mathrm{j}} = \frac{1}{\hat{\alpha}_j} \frac{\sum_{i=1}^{N} \gamma_{i,j} x_i}{\sum_{i=1}^{N} \gamma_{i,j}} \quad (6)$$

4. Go to step 2 until some tolerance is reached between consecutive iterations: $\left\|\boldsymbol{\Theta}^{(\mathbf{n})} - \boldsymbol{\Theta}^{(\mathbf{n-1})}\right\| < Tolerance$

Voxels are then designated as belonging to either the fat or muscle with certain probability as it is depicted in **Figure 5S** where the probability of belonging to pericardial fat, $p(Z_i = 1 | x_i, \Theta_1)$, is shown and the probability of being myocardial tissue is $p(Z_i = 2 | x_i, \Theta_2) = 1 - p(Z_i = 1 | x_i, \Theta_1)$. This probability is the information that guides both the probabilistic-driven initialization and the further deformation by considering vertices in the normal direction of the surface having the same probability of being pericardial fat and myocardial tissue. These sites demarcate the boundaries of the myocardial tissue. For this purpose the following weights are defined for each voxel in the normal direction:

$$w(x) = 1 - \frac{|p(Z_i = 2 | x_i, \Theta_2) - 0.5|}{0.5} \quad (7)$$

Note that these weights become 1 when the probability of being in the edge is higher (when $p(Z_i = 2 | x_i, \Theta_2) = 0.5$) and 0 when the voxel is entirely in the myocardial region or in the pericardial fat.

With these weights the orientation, scale and location of the heart model are recalculated according the weighted version of the Horn's quaternion-based algorithm [24].

The non-affine deformation is calculated as the weighted least squares solution obtained from the new set of candidates obtained from probabilistic-driven methodology as follows:

$$\boldsymbol{\Lambda}(\mathbf{b}) = (\boldsymbol{s} - \bar{\boldsymbol{s}} - \boldsymbol{\Phi}\mathbf{b})^{\mathbf{T}} \mathbf{W} (\boldsymbol{s} - \bar{\boldsymbol{s}} - \boldsymbol{\Phi}\mathbf{b}) \quad (8)$$

where $\boldsymbol{s}$ are now the candidate locations and $\mathbf{W}$ is a diagonal matrix whose elements are the weights obtained from the probabilistic characterization of the heart boundaries. We want to calculate the $\mathbf{b}$ coefficient vector that best fits the most likely candidates (those with weights equal to 1). The closed form solution is obtained by minimizing the function $\boldsymbol{\Lambda}(\mathbf{b})$resulting in:

$$\mathbf{b} = (\boldsymbol{\Phi}^{\mathbf{T}} \mathbf{W} \boldsymbol{\Phi})^{-\mathbf{1}} \boldsymbol{\Phi}^{\mathbf{T}} \mathbf{W} (\boldsymbol{s} - \bar{\boldsymbol{s}}) \quad (9)$$

So the new coefficients that represent the best fitting shape can be efficiently calculated with some matrix algebra.

Once the initialization is provided, the process automatically progress in a two-staged iterative fashion: first, the best affine transformation is found from the most likely candidates (**eq. 7**) then the non-affine deformation **b** is obtained **(eq. 9)**. This process iterates until the difference between sequential fittings is below certain tolerance: $\left\|\mathbf{b}^{(\mathbf{n})} - \mathbf{b}^{(\mathbf{n-1})}\right\| < Tolerance$. As a result, the boundaries of the manually initialized surface model depicted in Figure 2S are adjusted to reflect the myocardial surface. The result is a model of the myocardial surface of the heart (**Figure 6S**).

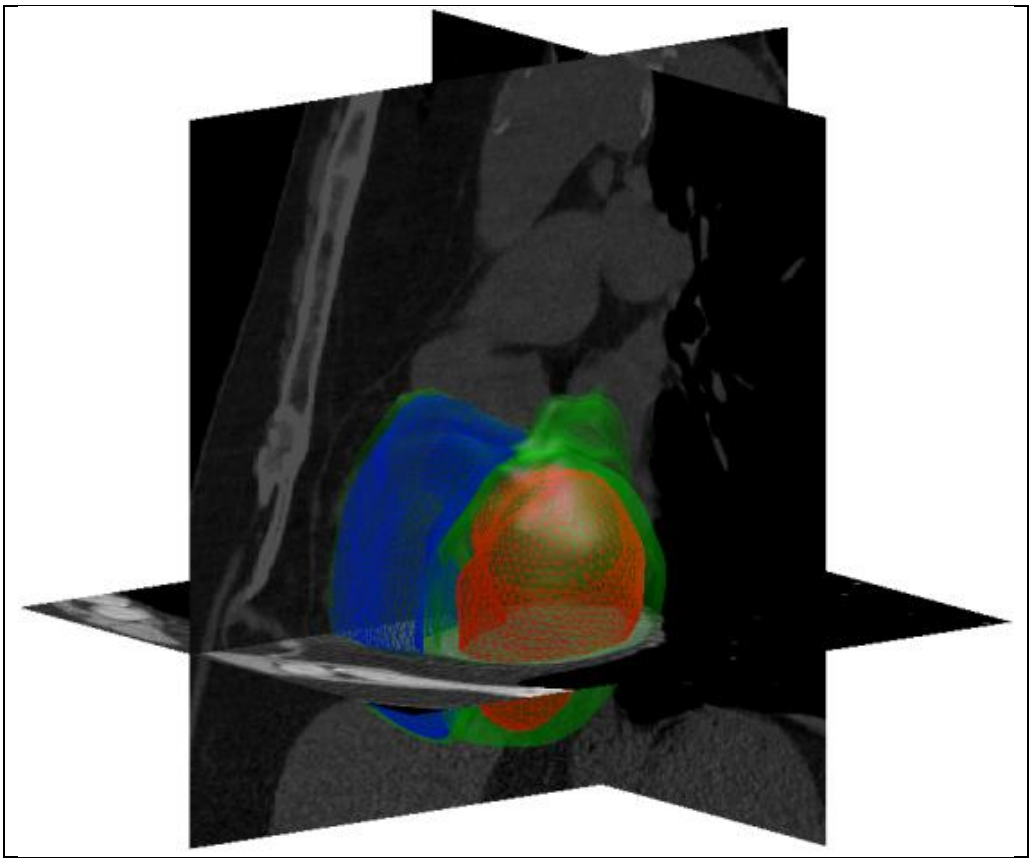

Figure 6S: Final myocardial segmentation

1. T. F. Cootes, C. J. Taylor, D. H. Cooper, J. Graham, Active shape models-their training and application. Computer vision and image understanding 61, 38 (1995).

2. B. K. P. Horn, Closed-form solution of absolute orientation using unit quaternions. Journal of the Optical Society of America A 4, 629 (1987).

3. G. Vegas-Sanchez-Ferrero, M. Martin-Fernandez, and M. J Sanches, in Multi-Modality Atherosclerosis Imaging and Diagnosis, L. Saba, Ed. (Springer, New York, 2014), pp. 155-171.

4. G. Vegas-Sanchez-Ferrero, A. A.-F. Tristan-Vega, S. ; Martin-Fernandez, M. ; Palencia, C.; Deriche, R. , in Biomedical Imaging (ISBI), 2012 9th IEEE International Symposium on (IEEE, Barcelona, 2012), pp. 1519-1522.